

Energetics of Technical Integration of 2-Propanol Fuel Cells: Thermodynamic and Current and Future Technical Feasibility

Katharina Braun,* Moritz Wolf, Ana De Oliveira, Patrick Preuster, Peter Wasserscheid, Simon Thiele, Lukas Weiß, and Michael Wensing

2-Propanol/acetone is a promising liquid organic hydrogen carrier system for fuel cell reactions. Herein, six different concepts for a 2-propanol/acetone fuel cell system are evaluated in MATLAB simulation with respect to their thermodynamic integration and technical feasibility. Four of the concepts use a direct 2-propanol fuel cell while the other two first release molecular hydrogen from 2-propanol and subsequently use a hydrogen fuel cell. The presented liquid phase 2-propanol fuel cell concept is thermodynamically feasible but cannot be realized technically using commercial Nafion membranes, due to membrane dissolution by the 2-propanol/acetone/water fuel mixture. Gaseous 2-propanol fuel cells imply a high heating requirement for the evaporation of the fuel. A direct high-temperature fuel cell using 2-propanol is thermodynamically feasible because there is less water in the overall system but is not technically feasible because of the esterification of phosphoric acid. A very interesting option is the conversion of gaseous 2-propanol to pressurized hydrogen in an electrochemical pumping step followed by a hydrogen fuel cell, because here the waste heat of a sufficiently hot hydrogen fuel cell can drive the 2-propanol evaporation.

1. Introduction

Due to the increasing importance of hydrogen as an energy carrier in the transition to fully renewable energy systems, alternative technologies to the expensive storage and transportation of pure elemental hydrogen are required. The liquid organic hydrogen carrier (LOHC) technology represents a promising method for the chemical storage of hydrogen and can make use of the existing energy infrastructure for liquid fuels. Hydrogen storage in the LOHC system proceeds via the reversible hydrogenation and dehydrogenation of organic molecules in repeatedly applied storage cycles without emitting CO₂.^[1] One prominent LOHC system is based on the dibenzyltoluene (H0-DBT)/perhydro-dibenzyltoluene (H18-DBT) couple: H0-DBT acts as a hydrogen-lean carrier. In an exothermic catalytic hydrogenation step, H0-DBT is loaded with


hydrogen and forms the hydrogen-rich carrier H18-DBT. This compound can release hydrogen in an endothermic catalytic dehydrogenation reaction. The released hydrogen can then be used directly in a fuel cell. The major advantages of the LOHC technology are hydrogen storage and transport in a liquid state with very high volumetric and comparatively high gravimetric energy densities under ambient conditions.

In general, it would be advantageous to combine the dehydrogenation and the fuel cell reaction in a single process step, i.e., to use the hydrogen-rich LOHC compound directly as fuel for a fuel cell. However, direct electrification of H18-DBT in fuel cells, has not been realized at an attractive performance level so far.^[2] Instead, it has been found that secondary alcohols, such as 2-propanol, are attractive fuels for direct electrification.^[3] Most interestingly, the dehydrogenation of 2-propanol in a proton exchange membrane (PEM) fuel cell setup stops at acetone and no CO₂ is formed.^[4] The resulting acetone can be recharged with hydrogen via catalytic hydrogenation^[5] or transfer hydrogenation.^[6] Sievi et al. demonstrated that transfer hydrogenation from H18-DBT to 2-propanol can be highly energy efficient (>50%). The hydrogen-rich H18-DBT releases hydrogen in contact with acetone, producing 2-propanol and the hydrogen-lean H0-DBT. By feeding the fuel cell with 2-propanol, acetone is formed, which in turn can be converted back into 2-propanol

K. Braun, L. Weiß, M. Wensing
Department of Chemical and Biological Engineering
Professorship for Fluid Systems Technology
Friedrich-Alexander-Universität Erlangen-Nürnberg
91058 Erlangen, Germany
E-mail: katharina.braun@fau.de

M. Wolf, A. De Oliveira, P. Preuster, P. Wasserscheid, S. Thiele
Helmholtz-Institute Erlangen-Nürnberg for Renewable Energy (IEK-11)
Forschungszentrum Jülich GmbH
91058 Erlangen, Germany

P. Wasserscheid
Department of Chemical and Biological Engineering
Friedrich-Alexander-Universität Erlangen-Nürnberg
91058 Erlangen, Germany

 The ORCID identification number(s) for the author(s) of this article can be found under <https://doi.org/10.1002/ente.202200343>.

© 2022 The Authors. Energy Technology published by Wiley-VCH GmbH. This is an open access article under the terms of the Creative Commons Attribution-NonCommercial-NoDerivs License, which permits use and distribution in any medium, provided the original work is properly cited, the use is non-commercial and no modifications or adaptations are made.

DOI: 10.1002/ente.202200343

through contact with the hydrogen-rich H18-DBT. Besides the main product acetone, hardly any side products, such as CO or CO₂ could be detected, since the C–C bond is not cleaved in the electrochemical oxidation of isopropanol to acetone.^[4] Fortunately, the heat level of the endothermic H18-DBT dehydrogenation corresponds approximately to the heat level of the exothermic acetone hydrogenation. Thus, no additional heat sources are required for the transfer hydrogenation.

With this approach of transfer hydrogenation as a thermo-neutral transformation, the combination of a transport-optimized LOHC with high energy density (H18-DBT/H0-DBT) and a fuel-cell-optimized LOHC with high-power density (2-propanol/acetone) is enabled. Encouraged by these results, Hauenstein et al. developed 2-propanol fuel cells with high-power densities (up to 254 mW cm⁻²).^[7] Furthermore, optimal configurations of the membrane electrode assembly were identified.^[8] However, no balance of plant (BOP) of a 2-propanol/acetone fuel cell system has been considered so far.

There are three different types of fuel cells available for 2-propanol electrification, which are at different levels concerning their technological development: 1) Low-temperature polymer electrolyte membrane fuel cells (LT-PEMFC) are operated in the temperature range between 60 and 90 °C. Due to the use of perfluorinated sulfonic acid (PFSA) ionomers, e.g., Nafion, as solid electrolyte, LT-PEMFCs require a high degree of hydration and show a significantly reduced performance above 100 °C.^[9] Commercially available Nafion-type perfluorosulfonic acid (PFSA)-based membranes are commonly used in fuel cell applications.^[10] LT-PEMFCs are currently the fuel cell types that are at the highest stage of development and are increasingly used in commercial automotive applications. 2) High-temperature PEM fuel cells (HT-PEMFC) use phosphoric acid (PA)-doped membranes based on polybenzimidazole (PBI).^[9] These membranes feature a different conduction mechanism compared to PFSA-type membranes that allow for effective fuel cell operation in a temperature range between 140 and 180 °C under anhydrous conditions.^[11] This means that the membrane does not need to be humidified for proton conduction. In addition, this type of fuel cell provides thermal energy at a comparatively high-temperature level, which is advantageous for heat recovery in a BOP. Currently, this fuel cell type is mainly considered for stationary applications. 3) For the medium temperature range between LT-PEMFC and HT-PEMFC, i.e., the temperature range between 100 and 140 °C, middle-temperature fuel cells (MT-PEMFC) operating with PFSA-based composite membranes are discussed.^[12–15] These composite membranes contain, for example, hydrophilic particles, to facilitate the water management of the membrane at relatively low humidity. It is fair to say, however, that at the current state of development the power density of these MT-PEMFC systems is low due to the decrease in PFSA conductivity at elevated temperatures.

In this study, the balance of plants for 2-propanol electrification is analyzed and different process configurations are compared. Note, that this comparison considers only the electrification of 2-propanol and does not take into account possible heat integration options that arise from the combination with a potential transfer hydrogenation process. 2-propanol itself represents the hydrogen-rich compound of the 2-propanol/acetone

LOHC couple. It is characterized by a hydrogen storage capacity of 3.33 mass% (864 Wh L⁻¹), an excellent technical availability, and a very attractive ecotoxicological profile.

In total, six different setups are considered: Four different temperature scenarios deal with the comparison of liquid and gaseous 2-propanol feeding and use a fuel cell operating with 2-propanol as fuel (one-step scenario). Two additional scenarios consider the thermal and electrochemical dehydrogenation of 2-propanol and the resulting hydrogen is used in a hydrogen fuel cell to generate electricity (two-step scenario), see **Figure 1**.

We evaluate two key characteristics of the different scenarios: The first characteristic is the thermodynamic integration capability of the different systems. On the basis of reasonable heat transfer calculations, it is evaluated whether a reasonable net energy may be generated in the one- or two-step scenarios. Second, the technical feasibility is considered based on the state of the art of the different scenarios. Based on these two characteristics, we are able to derive the roadmap which is currently most suitable to a technically relevant configuration of a 2-propanol/acetone fuel cell system. Likewise, the most important necessary improvements and developments concerning material for future research can be derived.

In Figure 1, the assessment of both thermal integration and technical feasibility is categorized in the form of a red/ orange/ green color code. Red indicates the presence of aspects that are certain to lead to unfeasibility, e.g., chemical behaviors or material problems at the current status. From a thermodynamic perspective this means concretely that either the energy balance of the fuel cell is negative and/or the whole system is not sustainable which would require an external heat source. Yellow markers show that there are some challenges that could be solved in the future. There are already technical improvements that are leading in the right direction but there are still some steps missing to categorize under feasibility. Thermodynamic feasibility cannot be categorized yellow. The green color indicates feasibility based on the simulations carried out in this article, which means a sustainable system, and the state-of-the-art described in the literature. All scenarios are discussed in detail in Section 3. **Table 1** shows all modeling assumptions for the operation and fuel cell parameters for each concept.

2. Methodology and Boundary Conditions

To compare different technical concepts, boundary conditions have to be set. These are based on certain assumptions whose validity is discussed in the following. The general boundary conditions are described in the following section and summarized in Table 1. Since we analyze experimental data in a range over 200 K, we assume that fluid properties are constant in this range.

The first boundary condition for all concepts is that the system runs in a steady-state operation. Furthermore, we assume that the system delivers a net electrical power of 250 W. This condition is derived from the idea of using a 2-propanol electrification process to power a small electric vehicle.^[16]

For the peripheral devices of the power system, such as fans, pumps, and controllers, we assume a power requirement of 200 W independently from the selected concept. Consequently, the overall system must provide at least a power

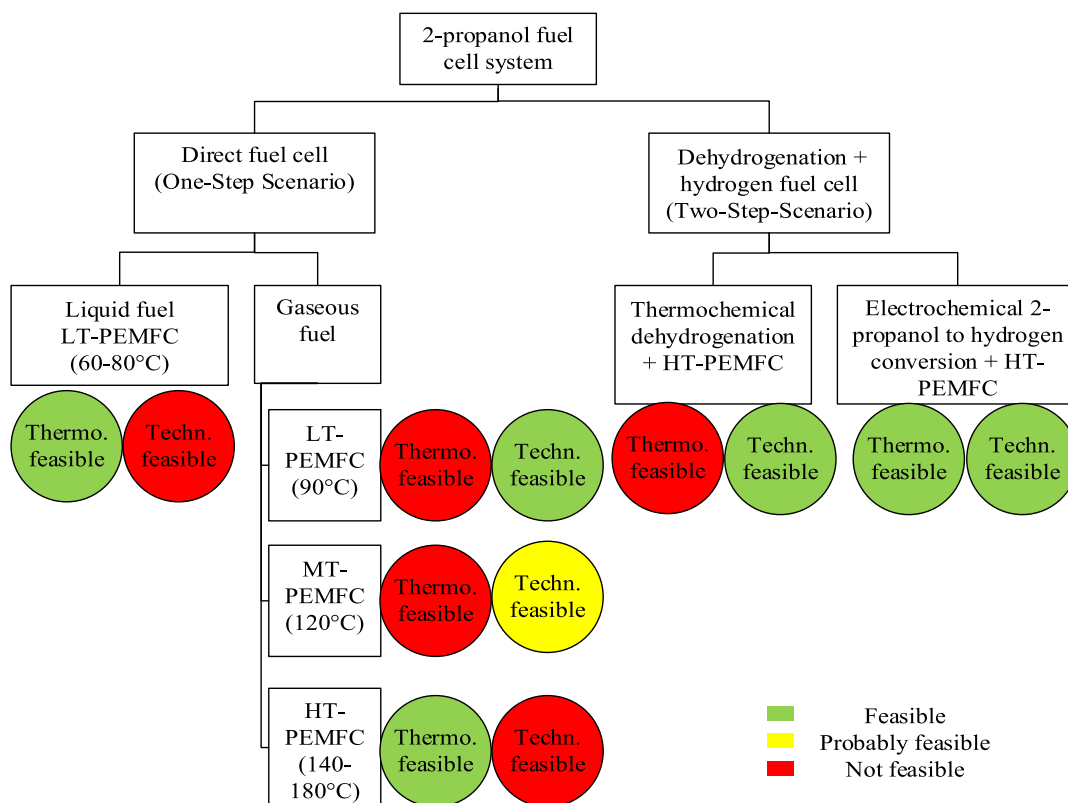


Figure 1. Overview of thermodynamic and technical feasibility of all scenarios.

Table 1. Modelling assumptions of operation and fuel cell parameters for each concept.

	Feed anode	Feed cathode (stoichiometry)	Exhaust cathode (relative humidity RH)	(fuel) utilization	System pressure	Fuel cell efficiency	Drag coefficient
Direct-LT-PEMFC, liquid	2 M aqueous 2-propanol solution	Air, No humidification 2.5	100% RH of the air	0.3	Ambient	0.5	4
Direct-LT-PEMFC, gaseous	87% 2-propanol, 13% water, evaporated	Humidified air 100% RH 2.5	100% RH of the air	0.55	Ambient	0.5	4
Direct-MT-PEMFC, gaseous	87% 2-propanol, 13% water, evaporated	100% RH of air at 99 °C At target temperature 120 °C: RH 51% 2.5	All water that exists on the cathode side is carried out by gaseous	0.55	Ambient	0.5 × 0.75 = 0.375 with less humidity at 120 °C Power density reduces	4
Direct-HT-PEMFC, gaseous	Pure 2-propanol, evaporated	Air, No humidification 2.5	All water that exists on the cathode side is carried out by gaseous	0.55	Ambient	0.5	–
Dehydrogenation + hydrogen HT-PEMFC	Pure 2-propanol, evaporated	Air, No humidification 2.5	All water that exists on the cathode side is carried out by gaseous	0.95 Recirculation	ambient	0.6	–
Electrochemical conversion + hydrogen HT-PEMFC	EHC: 2-propanol, evaporated FC: H ₂ , 1.5 bar	Air, No humidification of fuel cell, 2.5	EHC: humidified H ₂ FC: all water carried out	EHC: 0.8 FC: 0.95, recirculation	1.5 bar	0.6	–

of 450 W. It should be noted that the selected system performance is relatively low and the ratio of peripheral demand to total power is comparatively high. We assume that this ratio will be much lower in upscaling scenarios, which makes our approach rather conservative. However, as we will see, the main results of this study are relatively independent of system performance.

The system efficiency η_{system} is defined by the ratio of the net electrical power P_{net} and the chemical energy of the reacting fuel mass flow P_{chem}

$$\eta_{\text{system}} = \frac{P_{\text{electric}} - P_{\text{periphery}}}{P_{\text{chem}}} = \frac{P_{\text{net}}}{P_{\text{chem}}} \quad (1)$$

All systems considered here are open systems with respect to the 2-propanol feeding and acetone removal. Therefore, it makes more sense to define the system efficiency as a function of the mass flow of the reacting fuel and not of the fuel fed to the system as defined earlier. The 2-propanol stream is conditioned and introduced into the cell. The utilization of 2-propanol depends on the scenario but never reaches 100%. This means that there is still some residual 2-propanol in the exhaust stream of the cell. Thermodynamically, it would be attractive in any case to recirculate the heated (and humidified) exhaust gas stream. The influence of recirculation on the final result was found to be quite large.

In contrast, recirculation also increases the acetone content in the feed. Since no data was available on how the acetone content affects the utilization of the 2-propanol and the power density of the fuel cell, we decided not to consider recirculation any further in this study. At the same time, we think that using recirculation has great potential for the improvement of direct 2-propanol fuel cell concepts.

The ambient conditions were set to 15 °C, 30% relative air humidity (RH), and 1013.25 mbar air pressure. Air temperature and humidity have an impact on the overall performance of the system, as heating and humidifying the supply streams require energy. However, for a concept overview, these ambient conditions seem to be representative to analyze the advantages and disadvantages of the different concepts.

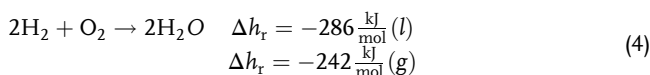
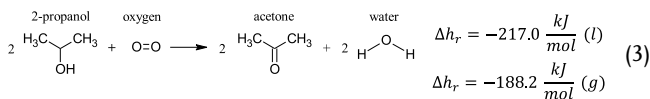
To compare the systems, our considerations and boundary conditions were implemented in a MATLAB/Simulink model. This model describes the enthalpy and mass flows as well as the heat transfer and energy conversion in the respective fuel cell system. The fuel cell system consists of the following subsystems: fuel cell, heat exchangers, humidifiers, and compressor/expander.

In the following, we will introduce the general thermodynamic modeling of these subsystems.

2.1. Fuel Cell

To describe the fuel cell subsystem, we apply the first law of thermodynamics by treating the specific heat and evaporation enthalpies of each inlet and outlet stream separately from their chemical potential, see Equation (2). The chemical potential refers only to the reaction enthalpy of the 2-propanol/acetone system or of the pure hydrogen when considering a hydrogen fuel cell, which is described in Equation (3) and (4). The associated boundary conditions were taken into account.^[17]

$$\dot{Q} + P_{\text{electric}} = \dot{m}_{\text{anode,in}} \times h_{\text{anode,in}} + \dot{m}_{\text{cathode,in}} \times h_{\text{cathode,in}} + \Delta \dot{H}_R - \dot{m}_{\text{anode,out}} \times h_{\text{anode,out}} - \dot{m}_{\text{cathode,out}} \times h_{\text{cathode,out}} \quad (2)$$



2.1.1. Energy and Mass Balance

In a fuel cell, the chemical energy flow $\Delta \dot{H}_R$ is converted into electrical power P_{electric} and a heat flow. Part of the heat is transported out of the system by the outlet gases on the cathode and anode side and contributes to their specific enthalpy h_{out} . The residual heat \dot{Q} is dissipated by the cooling system $\dot{Q}_{\text{cooling system}}$. In addition, a small part is lost due to non-ideal insulation $\dot{Q}_{\text{heat loss}}$. Consequently, \dot{Q} can be written as

$$\dot{Q} = \dot{Q}_{\text{cooling system}} + \dot{Q}_{\text{heat loss}} \quad (5)$$

The loss due to the nonideal insulation $\dot{Q}_{\text{heat loss}}$ was assumed to be 5% of the heat generated due to the electrochemical reaction.^[18]

$$\dot{Q}_{\text{heat loss}} = 0,05 \times \Delta \dot{H}_R \times (1 - \eta_{\text{fuel cell}}) \quad (6)$$

The electric power P_{electric} depends on the mass flow of the fuel \dot{m}_r participating in the reaction, the specific enthalpy of reaction h_r , and the fuel cell efficiency $\eta_{\text{fuel cell}}$, the latter having been assumed based on literature values and not further split up into different contributions.^[17]

$$P_{\text{electric}} = \Delta \dot{H}_R \times \eta_{\text{fuel cell}} = \dot{m}_r \times h_r \times \eta_{\text{fuel cell}} \quad (7)$$

It has already been mentioned in the previous section that the utilization of the fuel is scenario-dependent. Therefore, the required fuel feed $\dot{m}_{\text{fuel,in}}$ for the fuel cell was calculated based on the utilization X_{fuel} and the electric power demand.

$$\dot{m}_{\text{fuel,in}} = \frac{\dot{m}_r}{X_{\text{fuel}}} = \frac{P_{\text{electric}}}{X_{\text{fuel}} \cdot h_r \cdot \eta_{\text{fuel cell}}} \quad (8)$$

For the electrochemical reaction, the unconverted mass flow is irrelevant, but it must be kept in mind that the excess fuel $\dot{m}_{\text{ex}} = \dot{m}_{\text{fuel,in}} - \dot{m}_r$ must also be heated up or evaporated without recirculation. If this heat cannot be recovered, this has a negative effect on the efficiency of the system. From a thermodynamic point of view, high utilization is, therefore, desirable—just as it is from the point of view of overall system efficiency. This is the reason why the definition of the recirculation rate as well as the utilization affects the results of this study. Consequently, it is of great importance to select realistic values. For fuel utilization, this was possible because experimental data is available for the state of the art of membrane-electrode-assembly materials.

When considering the energy and mass balance, a crossover is neglected since it does not matter if the fuel is leaving the cell at

the anode or cathode side. This means all the fuel that does not participate in the reaction leaves the cell through the anode outlet and no nitrogen or oxygen is present on the anode side.

The mass flow of the cathode inlet $\dot{m}_{\text{cathode,in}}$ or rather the mass flow of air is directly proportional to the mass flow of the fuel taking part in the reaction and depends on the chemical equation. Taking a stoichiometric factor into account, the mass flow rate of the air can be determined. In the literature, a stoichiometric factor of 2.5 is typically used for the feed streams.^[15] This value was also assumed for the simulation in the context of this study. We will see that a small stoichiometric factor is always advantageous from a thermodynamic point of view. At the cathode, the mass flow rate of the air outlet is equal to that of the air inlet minus the oxygen consumed in the reaction.

The cathode inlet and outlet streams are treated as humid air. The specific enthalpy of humid air h_{1+x} is the heat content of the air–water vapor mixture, related to the mass of dry air. The enthalpy of humid air is defined based on the specific heat capacity of dry air $c_{p,l}$, the temperature T , the water content X , the enthalpy of evaporation of the water h_v , and the specific heat capacity of the water vapor $c_{p,w}$.^[19] If the air is saturated and liquid water is present, the third part of the formula with the water content in the saturation state X_s and the specific heat capacity of liquid water $c_{p,f}$ must be taken into account.^[20]

$$h_{\text{cathode}} = h_{1+x} = c_{p,l} \times T + X_s \times (h_v + c_{p,w} \times T) + (X - X_s) \times c_{p,f} \times T \quad (9)$$

Consequently, the specific enthalpy of the cathode inlet and outlet streams $h_{\text{cathode,in}}$ and $h_{\text{cathode,out}}$ can be calculated based on their temperature and water content according to Equation (9). The water content X depends on partial pressure p_w and total pressure p (Equation (10)).

$$X = 0.622 \times \frac{p_w}{p - p_w} \quad (10)$$

The partial pressure can be calculated from the relative humidity ϕ and the saturation pressure $p_s(T)$.^[21]

$$p_w = p_s(T) \times \phi \quad (11)$$

With higher total pressure at constant temperature and constant mixing ratio, the partial pressure and the relative humidity increase.

For temperatures above 100 °C, the enthalpy of the air leaving the fuel cell is calculated, considering dry air and water as two separate mass flows

$$\dot{H}_{\text{air,out}} = \dot{m}_{\text{air}} \times c_{p,l} \times T + \dot{m}_{\text{water}} \times (c_{p,w} + h_v) \times T \quad (12)$$

The mass flow of water \dot{m}_{water} is determined by the water balance, assuming a balance of zero, which means that no water accumulates in the fuel cell. The water balance is described in detail in the next section.

The specific enthalpies for the anode streams were calculated analogously to the cathode side, but using the fluid properties of the respective carrier medium: 2-propanol, acetone, or hydrogen.

2.1.2. Water Balance

Water plays a significant role in a polymer electrolyte membrane fuel cell because it increases the conductivity of the protons through the membrane. In contrast, too much water can flood the fuel cell and cause a decrease in power. For this reason, it is necessary to control the water balance in the fuel cell.^[22] As a look at the simulation results reveals, the amount of water is also important from a thermodynamic point of view. Compared to 2-propanol, water has 3.7 times the enthalpy of evaporation (per mass). Therefore, it has a significant influence on the energy balance of the fuel cell. **Figure 2** shows the water balance in our fuel cell model.

Water is introduced into the cell via the air on the cathode side and, depending on the operating scenario of the fuel cell, additionally on the anode side. The water on the cathode side is equal to the water content of the air. The amount of water on the anode side depends on the solution or gas mixture fed into the cell. The water that is produced during the reaction also accumulates in the cathode. During the transport of the protons through the membrane, water molecules are dragged from the anode to the cathode.^[10] The electro-osmotic drag coefficient n_{drag} indicates, how many water molecules $n_{\text{H}_2\text{O}}$ are moved by one hydrogen proton H^+ .

$$n_{\text{drag}} = \frac{n_{\text{H}_2\text{O}}}{\text{H}^+} \quad (13)$$

In this study, the drag coefficient is assumed to be constant with a value of 4.^[10]

Due to the concentration gradient of water in a fuel cell, water diffuses back to the anode. Since the fuel was mixed with water, the concentration gradient is very small, and back diffusion thus was neglected in this work. The water at the cathode outlet can be determined under the condition that no water accumulates in the cell. In low-temperature fuel cells, the amount of water at the cathode outlet is limited by the saturation of the air. It is assumed that the air carries as much water as it can absorb, i.e., a relative humidity of 100%.

2.2. Heat Exchanger

To design a thermodynamically efficient system, thermal management is the key. Therefore, heat exchangers must be used to recover waste heat from the fuel cell outlet streams to

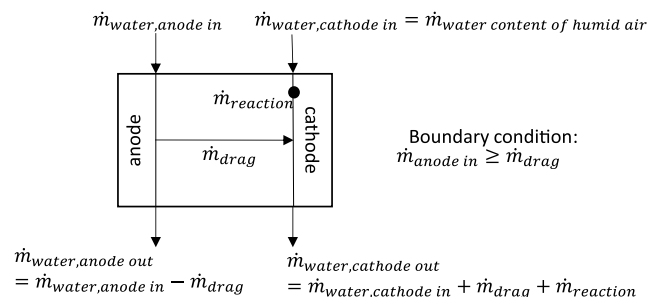


Figure 2. Water balance of our fuel cell model.

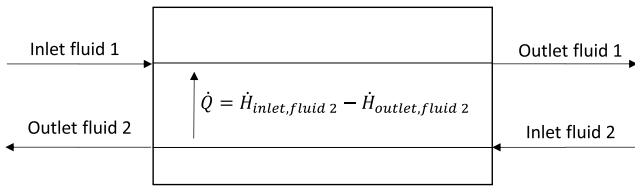


Figure 3. Heat transfer from fluid 2 to fluid 1 in a counter-flow heat exchanger.

heat and evaporate the inlet streams. Two heat sources are available: the cooling circuit and the exhaust gases.

To evaluate whether heat exchange is possible in different scenarios, three crucial system constraints were defined. If all these conditions are met, a technical realization of the heat exchanger should be possible.

First, there must be a sufficient heat flow \dot{Q} between the warmer fluid 2 and the colder fluid 1 to reach the temperature needed for the outlet of fluid 1 (**Figure 3**).

This leads to the following condition

$$\frac{\dot{H}_{\text{outlet,fluid1}} - \dot{H}_{\text{inlet,fluid1}}}{(\dot{H}_{\text{inlet,fluid2}} - \dot{H}_{\text{outlet,fluid2}}) \times \eta_{\text{heat exchanger}}} < 1 \quad (14)$$

Since the heat transfer in a heat exchanger is not ideal, an efficiency of the heat exchanger $\eta_{\text{heat exchanger}}$ of about 90% was assumed, based on realistic values for counter-flow heat exchangers from the literature.^[23] This means that the heat released from fluid 2 must be higher than the heat required for heating or evaporating fluid 1. The total heat flow \dot{Q} between the hot and the cold fluid can be expressed considering the enthalpy flows \dot{H} . These are functions of the mass flow \dot{m} , the specific heat capacity of the fluid $c_{p,\text{fluid}}$, and the temperature difference ΔT , which is defined by the inlet and outlet temperature of the heat exchanger. Due to phase transition, a latent heat term for the evaporation enthalpy $h_{v,\text{fluid}}$ must be added. Thus, the following equation applies to the enthalpy flow^[23]

$$\dot{H}_{\text{fuel}} = \dot{m}_{\text{fluid}} \times (c_{p,\text{fluid,liquid}} \times \Delta T + h_{v,\text{fluid}}) \quad (15)$$

Furthermore, the inlet temperature of fluid 2 always has to be higher than the outlet temperature of fluid 1 (**Figure 4**). This results in Equation (16).

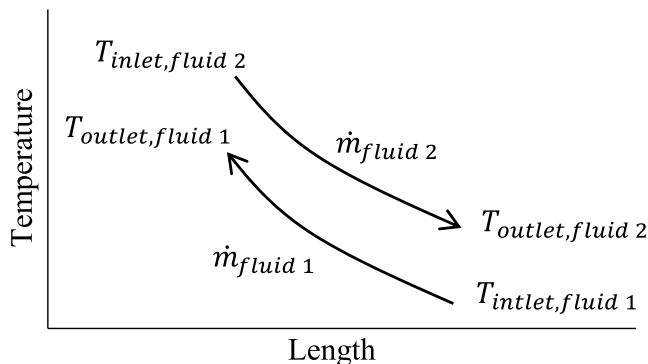


Figure 4. Temperature profile of a counter-flow heat exchanger.

$$T_{\text{inlet, fluid2}} > T_{\text{outlet, fluid1}} \quad (16)$$

Regarding the design of a heat exchanger, the heat flow transferred in the heat exchanger (considering incompressible fluids and isobaric conditions) is defined as

$$\dot{Q} = k \times A \times T_m \quad (17)$$

k is the heat transition coefficient, A is the heat transition surface area, and T_m is the mean logarithmic temperature difference.^[24]

For the design of a heat exchanger, this equation means that the smaller the temperature difference, the larger the heat transfer area must become, while the transferable heat flow remains constant since the heat transfer coefficient can hardly be influenced.

For the heat exchanger to remain within an applicable size, the mean logarithmic temperature difference should not become too small. Therefore, a value of 5 K was assumed. This results in the third condition

$$T_m = \frac{(T_{\text{exhaust,in}} - T_{\text{fuel,out}}) - (T_{\text{exhaust,out}} - T_{\text{fuel,in}})}{\ln\left(\frac{T_{\text{exhaust,in}} - T_{\text{fuel,out}}}{T_{\text{exhaust,out}} - T_{\text{fuel,in}}}\right)} > 5 \text{ K} \quad (18)$$

2.3. Humidifier

In PEM-fuel cells, the air must be humidified before entering the flow field to enable sufficient proton conductivity of the membrane. There are various possibilities for external as well as internal humidification.^[25] However, according to Peng et al.^[26] the operating principle of a membrane humidifier was considered the most feasible and energy-efficient strategy in the context of this study. A membrane humidifier basically works like a heat exchanger, but in addition to heat, it can also transfer water over the membrane.

Applying this concept to our system requires no external water supply, as the humid exhaust air can be reused to heat and humidify the inlet air. The only condition is that enough water is provided by the cell to humidify the inlet air.

$$\dot{m}_{\text{water, cathode, out}} > \dot{m}_{\text{water, cathode, in}} \quad (19)$$

Since the air leaving the fuel cell is warmer than the air entering it, more water can be transported out of the fuel cell than into it. The aforementioned condition is, therefore, fulfilled in all concepts considered in this study.

2.4. Compressor/Expander

Concepts with higher system pressure than ambient require a compressor and an expander. The temperature and work in these devices can be calculated according to the polytropic process^[20]

$$T_2 = \left(\frac{p_2}{p_1}\right)^{\frac{\kappa-1}{\kappa}} \times T_1 \quad (20)$$

$$w_{1-2} = \frac{\kappa}{\kappa-1} \times R \times T_1 \times \left(\left(\frac{p_2}{p_1}\right)^{\frac{\kappa-1}{\kappa}} - 1 \right) \quad (21)$$

The polytropic exponent κ can be assumed to be constant and is 1.4 for air. p_1 and p_2 are the pressures and T_1 and T_2 are the temperatures before and after compression. w_{1-2} is the work.

$$P = \frac{w_{1-2} \cdot \dot{m}}{\eta_{\text{compr}} M} \quad (22)$$

The electric power requirement depends on the work w_{1-2} , the mass flow of air \dot{m} , the molar mass M and the compressor efficiency η_{compr} , which is assumed to be 0.7.^[27] An expander is needed to recover some of the energy when the air is released into the environment. The expansion can be calculated according to the compression. The efficiency of the expander is also assumed to be 0.7.^[27]

3. Results and Discussion of Scenarios

In this section, the various process configurations that were roughly presented in Figure 1 are described in detail. We will first present the one-step scenarios in which 2-propanol is fed directly into the fuel cell in either liquid or gaseous form. After that, the two-step scenarios in which 2-propanol is first dehydrogenated and then hydrogen is fed into the fuel cell are discussed. For a quick overview, each configuration is introduced showing the respective flow and Sankey diagrams. The flow diagrams contain all components that are relevant for the MATLAB/Simulink model and show how the process units are connected. The Sankey diagrams illustrate the energy flows from one component to another within the respective systems.

3.1. Direct Fuel Cell

Unless stated otherwise, the fuel cell efficiency was assumed to be 50%.^[28] All direct fuel cell concepts do not contain recirculation of the fuel, as discussed previously. Recirculation could improve efficiency if a technically reasonable implementation was possible. Therefore, an open system is considered with 2-propanol input and 2-propanol/acetone mixture output. The chemical reaction taking part in the direct fuel cell is according to Equation (3).

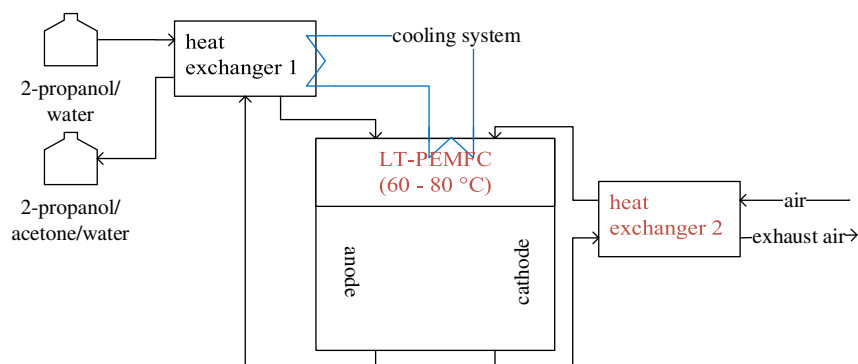


Figure 5. Flowchart including the main components for a direct fuel cell—LT-PEMFC with liquid 2-propanol/water feed.

3.1.1. Liquid Fuel—LT-PEMFC

The simplest and most straightforward way for a 2-propanol fuel cell system seems to be the direct feeding of a low-temperature PEM fuel cell with liquid 2-propanol.

Figure 5 shows the concept. A 2-propanol-water solution is fed from a tank via heat exchanger 1. In the literature, a 2 M aqueous solution is recommended as higher 2-propanol concentrations lead to damage of the MEA with current membrane material.^[3] In heat exchanger 1, the 2-propanol-water solution is heated but not evaporated. The heat can be recovered from the exhaust gas stream or the cooling system that transfers the waste heat from the fuel cell. The heated 2-propanol-water mixture flows into the fuel cell. The utilization of fuel is assumed to be 30%. Sievi measured a utilization of 55% in a vapor feed direct fuel cell,^[29] thus the assumed degree of fuel utilization is considered to be realistic and conservative. 2-Propanol that is not involved in the reaction, is discharged at the anode, as is the acetone produced. This discharge stream is cooled in heat exchanger 1 to transfer heat to the feed of the fuel cell.

Heated air is introduced at the cathode. Due to the liquid operation and high water content at the anode, it is possible to operate without humidifying the air at the cathode. At the cathode outlet, the air exits with fuel cell operating temperature and up to 100% humidity. The water release via the cathode exhaust gas is maximized when the humidity in the exhaust gas reaches 100%. This depends on the temperature and the vapor pressure. The relative humidity, in turn, is less than 100% if there is not enough water in the cell. Heat exchanger 2 transfers the heat from the fuel cell outlet air to the fuel cell inlet air.

First, the model assumptions and operating parameters were determined according to Table 1. Varying the input parameters of the model, the influence of various parameters was analyzed with regard to achieving a positive energy balance of the fuel cell and a net system power of 250 W.

A closer look at the energy balance of the liquid fuel cell shows that the amount of water has a major influence on the inlet and outlet enthalpy flows. Since a relatively large amount of water is supplied to the anode, whose temperature is below the operating temperature of the cell, and leaves the cell at operating temperature without participating in the reaction, an enthalpy deficit occurs in the cell. The fuel cell would have to be heated with almost twice the net power (at an operating temperature of 65 °C) to reach an

energy-neutral balance of the cell. The water plays a role not only on the anode side but also on the cathode side. The supplied air is only heated and not humidified, and the exhaust air is assumed to be saturated with water, as the air strives to absorb the maximum amount of water possible. Therefore, the enthalpy flow of the exhaust air is six times greater than that of the supplied air, which also means an energy deficit in the fuel cell.

Two main influencing parameters can be identified to solve these problems: 1) One aspect is lowering the stoichiometry so that less water is removed with the cathode air and thus a lower enthalpy flow leaves the cell. Considering the operating temperature range of the LT-PEMFC (60–90 °C), this means that it is even more important to lower the stoichiometry at higher operating temperatures of the fuel cell, as higher temperatures lead to higher water content in the air outlet stream. From a thermodynamic point of view, it is, therefore, better to operate at lower temperatures. From an electrochemical point of view, however, it is better to operate at higher temperatures where higher power densities can be achieved. 2) Another aspect is reducing water in the anode feed. A 4 M solution would result in an energy-neutral balance. Consequently, any more concentrated 2-propanol solution would result in an energy positive balance of the cell.

Taking the balance of the plant into account at this modified operating point (stoichiometric factor at the cathode: 1.2, anode

feed: 4 M solution), this concept achieves a system efficiency of 28% according to Equation (1). The required heat can be recovered in heat exchanger 1 to heat the fuel and in heat exchanger 2 to heat the air. To heat the 2-propanol solution to a few degrees below the operating temperature of the cell, heat is transferred from the exhaust stream mixture of 2-propanol, acetone, and water. To heat the inlet air, heat is transferred from the exhaust air to the supply air. A Sankey diagram shows the energy conversion of the entire system and provides a better impression of the effects of the different energy flows (Figure 6).

One issue that becomes clear is the impact of the utilization of the fuel. Since the utilization of fuel is only 30%, 70% of the chemical energy provided by the mass flow of the fuel cannot be converted into electrical energy, leaving the fuel cell unused. However, all the fuel must be heated and the entire system must be designed for these mass flows. With this concept, a net power of 250 W can even be achieved at a low utilization rate of 30%. Nevertheless, a higher fuel utilization would contribute significantly to a higher energy density and reduce the mass flow of the system. The input mass flow rate is about 0.83 g s^{-1} 2-propanol and 3.449 g s^{-1} of water for electrical power of 450 W.

In summary, this concept shows a thermodynamically possible way to use 2-propanol in a direct fuel cell, provided the anode feed is a 4M solution or higher.

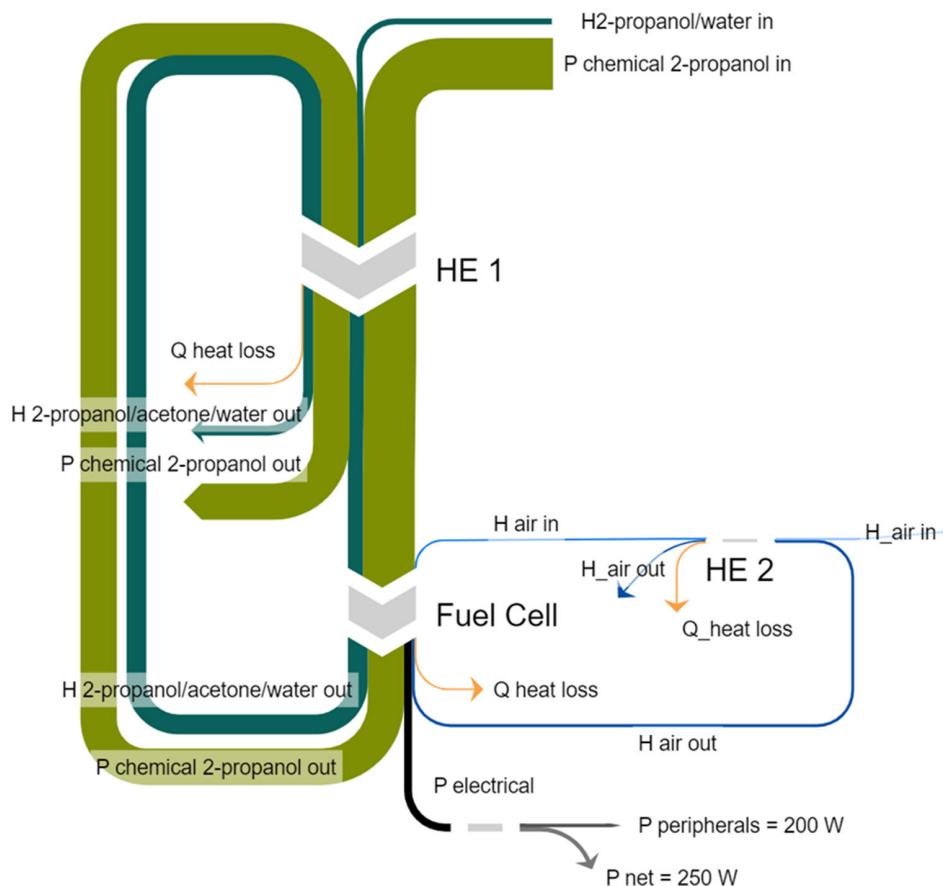


Figure 6. Energy flowchart of the whole system for a direct liquid low-temperature fuel cell with the components heat exchanger 1 (HE1) for the anode feed, heat exchanger 2 (HE2-vaporization) for the cathode feed, and fuel cell.

From a technical point of view, it is not yet possible to use these concentrations. Cao and Bergens reported destruction of the MEA due to excessive membrane swelling, dissolution of the recast PFSA in the catalyst layer, and electrode delamination when molar quantities higher than 2 M are used.^[30] This means there is a need for novel ionomer binders that are chemically stable in the presence of 2-propanol and acetone.^[3]

3.1.2. Gaseous Fuel

To avoid the dissolution of the conventional MEA membrane material by liquid fuel, evaporated 2-propanol can be fed to the fuel cell. It has been shown in the past that conventional MEA membrane materials are stable and remain fully functional in presence of 2-propanol/acetone/water vapor mixtures.^[3] Perry and Young found that at 85 °C the performance of a 2-propanol fuel cell operating with gaseous fuel increases when the water content is also increased.^[31] This is consistent with Sievi's results: He showed that the power is significantly lower without water in the gaseous anode feed.^[29] For the calculation of this study, the 2-propanol–water mixture was set to 87 wt% 2-propanol as applied in Sievi's experiments. At this mixing ratio, 2-propanol and water form an azeotrope mixture with a boiling temperature of 80.4 °C.^[32]

To feed gaseous 2-propanol to the fuel cell, heat recovery within the system is absolutely necessary, as the heat requirement of 2-propanol evaporation is quite high. There are basically two options for heat integration: 1) The use of waste heat from the fuel cell meaning that the heat is dissipated via a cooling medium and transferred to the fuel via a heat exchanger. 2) The recovery of heat from the fuel cell exhaust in a heat exchanger to vaporize the fuel. In both cases, the fuel cell operating temperature must be higher than the boiling temperature of the 2-propanol–water mixture (see Section 2.2).

LT-PEMFC: For the operation of a low-temperature PEM fuel cell with gaseous fuel, humidification of the cathode air is required, which can be realized by recovering water from the exhaust air using a membrane-based humidifier.^[25] The modeling of the humidifier is described in Section 2.3.

In this scenario, the fuel is heated to boiling temperature using the exhaust gas heat of the anode. The evaporation enthalpy should be provided by the waste heat of the fuel cell

(**Figure 7**). Therefore, the fuel cell temperature was set to the maximum value of 90 °C.^[10] The utilization is set to 55% according to Sievi's experimental studies.^[29]

The water balance is assumed to be the same as in the liquid phase configuration, with the exception of the cathode inlet. The cathode air is assumed to be 100% humidified in the present case assuming that sufficient water can be transferred to the humidifier.

Under these conditions, the simulation shows a positive energy balance of the fuel cell, but not of the whole fuel cell system. The waste heat of the fuel cell is about 292 W.

Further consideration of this concept shows an exceedingly high heat requirement for evaporation compared to the electrical energy generated. For the evaporation of the fuel–water mixture alone, a heat power of 740 W is required for a system with a net electric output of 250 W. This means that the waste heat is not sufficient for evaporation. Even if it were sufficient, this would not change much because it is technically difficult to transfer heat with such a small temperature difference of 9.6 K (90 to 80.4 °C). The option of recovering heat by cooling the exhaust gases shows the same challenge: Due to the small temperature difference, only a small part of the fuel–water mixture can be evaporated. Larger temperature differences would help to transfer more heat, but this would require to operate the fuel cell significantly above 90 °C.

In summary, it is thermodynamically impossible to evaporate the 2-propanol–water mixture with the heat of the exhaust gas or the waste heat of a fuel cell operating at 90 °C. The Sankey diagram below illustrates this conclusion (**Figure 8**).

Thus, evaporating 2-propanol/water using waste heat from a low-temperature fuel cell is not feasible energetically under the conditions considered in this paper. From a technical point of view, the operation of a low-temperature fuel cell with gaseous 2-propanol is possible and well-established, as mentioned in Section 1.

MT-PEMFC: In this scenario, a middle-temperature fuel cell is applied instead of a low-temperature one. In this way, a higher temperature gradient for heat transfer and vaporization of the fuel is envisaged. In addition, there are other benefits such as improved kinetics in the electrochemical conversion unit and facilitated cooling. Again, the heat can be recovered from the fuel cell exhaust or from fuel cell cooling (**Figure 9**).

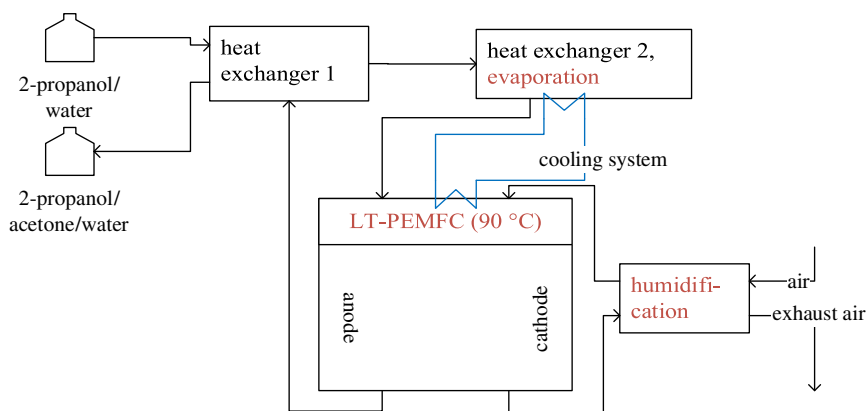


Figure 7. Flowchart including the main components for a direct fuel cell—LT-PEMFC with gaseous 2-propanol/water feed.

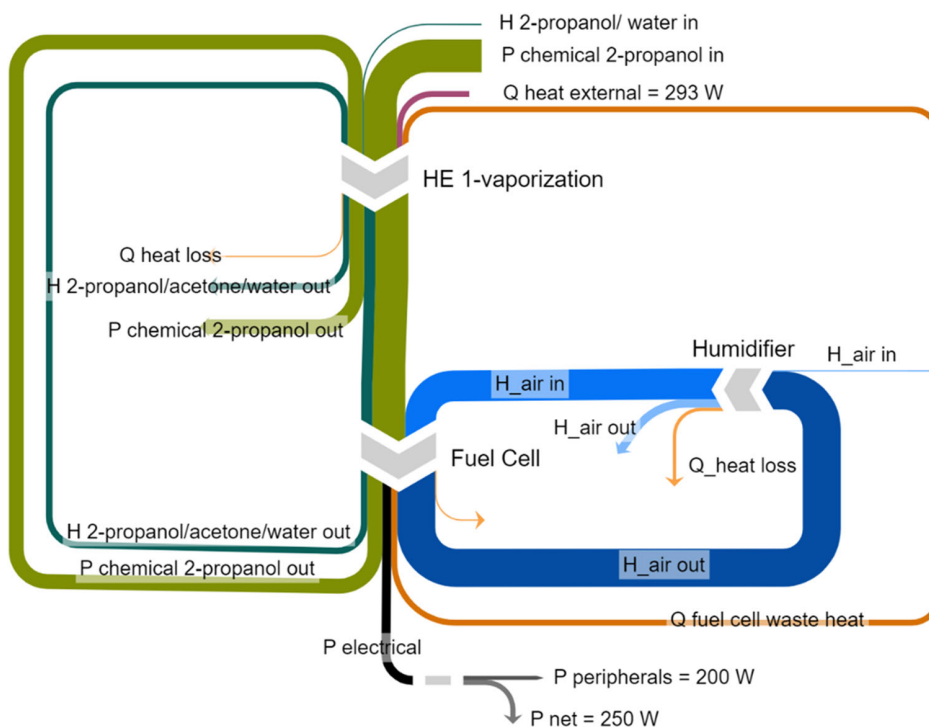


Figure 8. Energy flowchart of the whole system for a direct gaseous low-temperature fuel cell with the components heat exchanger 1 (HE1-vaporization) for the anode feed, humidifier for the cathode feed, and fuel cell.

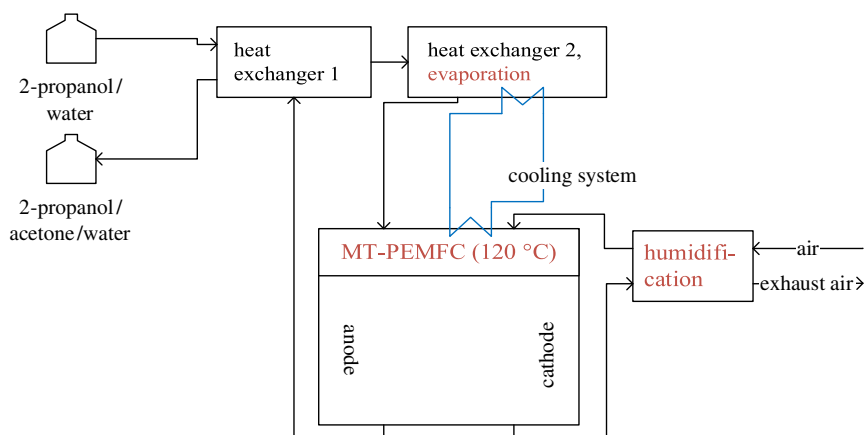


Figure 9. Flowchart including the main components for a direct fuel cell—MT-PEMFC with gaseous 2-propanol/water feed.

The fuel cell is fed with a vaporized fuel–water mixture with a 2-propanol content of 87 wt%, and a utilization of 55% is assumed as with the LT-PEMFC. To operate the fuel cell at elevated temperatures of up to 120 °C, the thermal and mechanical stability of PFSA must be improved. Various composite membranes with additives such as TiO₂, ZrP, or SiO₂ have been developed to increase the operating temperature. Nafion HP, a membrane reinforced with perfluorosulfonic acid /PTFE copolymer, is an example of a commercial product. In a recent study, higher power densities were achieved by direct membrane deposition compared to the use of Nafion HP membranes.^[15] However, the power densities decrease sharply with increasing

temperature due to the reduced wetting of the membrane and the resulting decrease in protonic conductivity. The maximum power density of the cell at 120 °C for the direct-deposited composite membrane fuel cell is only about 75% of the power density at 80 °C. The operating conditions are 95% relative humidity for the lower temperature and 35% relative humidity for the higher temperature at atmospheric pressure.

To avoid this drop in power density, the relative humidity at 120 °C must be increased. This is only possible with a higher system pressure than ambient, as the saturation pressure at 120 °C is 1985.36 mbar. The advantage of the higher pressure is that the water in the cell is still present in a liquid state to keep the

membrane humidified. This means that a compressor would be required to pressurize the cathode gas. To have comparable pressure on both sides of the membrane, the anode must also be pressurized. The negative effect is that the boiling temperature of the fuel increases with increasing pressure, which in turn leads to a lower temperature gradient between the operating temperature of the fuel cell and the boiling temperature. This leads to the same problem as in the previous scenario with the low-temperature fuel cell, namely that the temperature gradient is too small to vaporize the fuel.

This is why the concept is calculated with ambient system pressure and, in consequence, low relative humidity, which leads to lower power densities. Assuming that the power density decreases by 25% at 120 °C as explained earlier, the mass flow taking part in the reaction must increase to achieve the target power of 250 W. Lower power densities can also be compensated by higher cell areas, but for comparability with the other concepts, this parameter cannot be changed as it is not modeled.

The modeling of the water balance differs in one aspect: since the operating temperature is above 100 °C, all the water is gaseous. It is assumed that all the water that accumulates on the cathode side is removed with the dry air, so that the water balance is neutral.

The simulation shows a very high energy deficit of the fuel cell, which is required in the form of heat. This means that the fuel cell cools down during operation under the assumed conditions. Contrary to what might be expected, the fuel cell does not need to be cooled but heated. The amount of water in the air has the greatest influence. It is assumed, that the air inlet stream has a relative humidity (RH) of 100% at 99 °C, which means a high water load. Since the water accumulates on the cathode side and the outlet is a gas mixture of water and air, a large part of the water leaves the cell in the gas phase. Since the enthalpy of evaporation of water is 3.7 times higher than that of 2-propanol, the effects on the energy balance are much more serious than those of 2-propanol. This is one reason why this concept does not work from a thermodynamic point of view.

A look at the heat exchanger shows that the heat of the anode exhaust gas is not sufficient to heat the fuel. Taking the different boiling temperatures of the fuel–water–acetone mixture into account, it is technically impossible to evaporate the fuel–water solution in a heat exchanger without additional heating.

The recovery of waste heat was mentioned as a second possibility. But as stated earlier, the fuel cell has no positive energy balance. So there is no other heat source to manage the evaporation without external heat input. Even by varying the parameters, no operating point was found at which the energy balance of the fuel cell is positive.

In the case of the humidifier, it is possible to operate it without an additional energy supply, as the air outlet of the fuel cell can deliver sufficient heat and water to the inlet air.

The following diagram shows the energy balance of the direct fuel cell system with a middle-temperature fuel cell. The stoichiometry has already been reduced to 1.3, but both the fuel cell and the heat exchanger must be heated externally with a power that is 11 times higher than the usable electrical power of 250 W. In the energy flow diagram, the large influence of the humidified cathode air can clearly be seen. The enthalpy current of the cathode air leaving the fuel cell is higher than that of the air entering

because more water is removed than supplied. This big difference cannot be compensated by the heat of the reaction which is produced in the cell (**Figure 10**).

Thus, a 2-propanol fuel cell system cannot be made thermodynamically efficient with a direct middle-temperature fuel cell.

From a technical point of view, the scenario with a middle-temperature fuel cell is not readily feasible either. As mentioned above, the power density drops drastically due to lower humidification of the membrane, making MT-PEMFCs a current area of research struggling with much lower efficiency than current LT-PEMFCs (e.g., Refs. [33,34]).

HT-PEMFC: In this section, high-temperature fuel cells are evaluated. Since they have phosphoric acid (PA)-doped polybenzimidazole (PBI)-based membranes and operate between 140 and 180 °C, humidification is no longer required. **Figure 11** shows a flow diagram of the system.

The simulation model is similar to the MT-PEMFC model, except for the heat exchanger on the cathode side, which takes into account that the air does not need to be humidified. This leads to a lower amount of water in the cell as the humidity of the ambient air is assumed to be 30%. Pure 2-propanol is assumed as the gas feed. The electro-osmotic drag coefficient is assumed to be zero.^[35]

Under the assumed conditions, the fuel cell has a positive energy balance at both 140 °C (349.2 W) and 180 °C (299.3 W). If one compares the heat flow that can be transferred in the heat exchanger through the anode outlet flow of the fuel cell with the heat requirement needed to heat up and vaporize the fuel inlet, it turns out that there is not enough heat for vaporization. Moreover, the heat flow for heating up to boiling temperature is only high enough above a cell temperature of 170 °C. The enthalpy still required must be provided by the waste heat of the fuel cell. It varies with the operating temperature of the fuel cell. Higher temperatures mean higher outlet enthalpy currents and less waste heat as a consequence. In this respect, the lower point of the temperature range of a high-temperature fuel cell seems to be the more efficient one. By lowering the stoichiometric factor on the cathode side, the enthalpy flow at the air outlet can also be reduced. Finally, an operating point can be found at which the system operates quite efficiently. It is assumed that the very small heat deficit during evaporation is covered by the electrical energy of the fuel cell. This leads to a reduction in the efficiency of the entire fuel cell system, but it is still possible to achieve a positive net electrical balance. The energy flow diagram below shows the operating point at a fuel cell temperature of 140 °C, a stoichiometric factor of 1.3, a fuel cell efficiency of 50%, and a utilization of 55% (**Figure 12**).

Compared to the middle-temperature fuel cell, the high-temperature fuel cell has a major advantage: There is almost no water in the system. This leads to less heat dissipation of the fuel cell by water and to a positive energy balance of the fuel cell and ultimately to a positive energy balance of the entire system. The system efficiency at the given conditions is 0.165.

From a thermodynamic point of view, this concept seems feasible. From a technical point of view, there are some problems with the materials when using 2-propanol as fuel. As mentioned above, polybenzimidazole-based membranes doped with phosphoric acid are often used in polymer

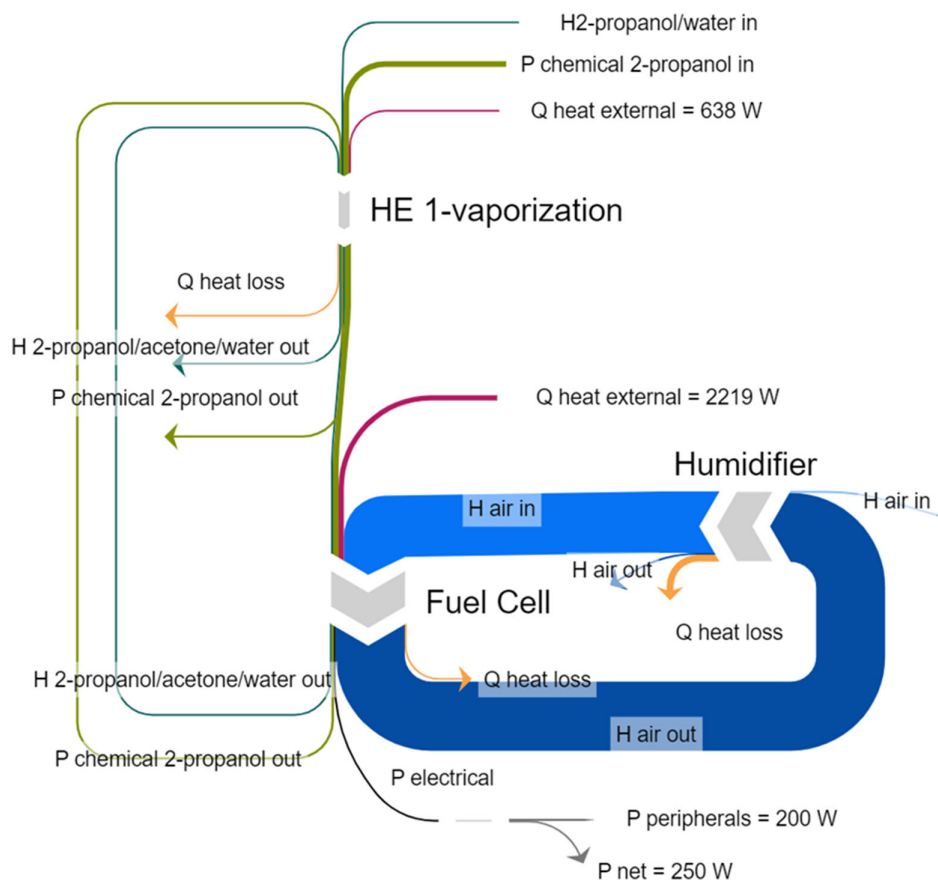


Figure 10. Energy flowchart of the whole system for a direct middle-temperature fuel cell with the components heat exchanger 1 (HE1-vaporization) for the anode feed, humidifier for the cathode feed, and fuel cell.

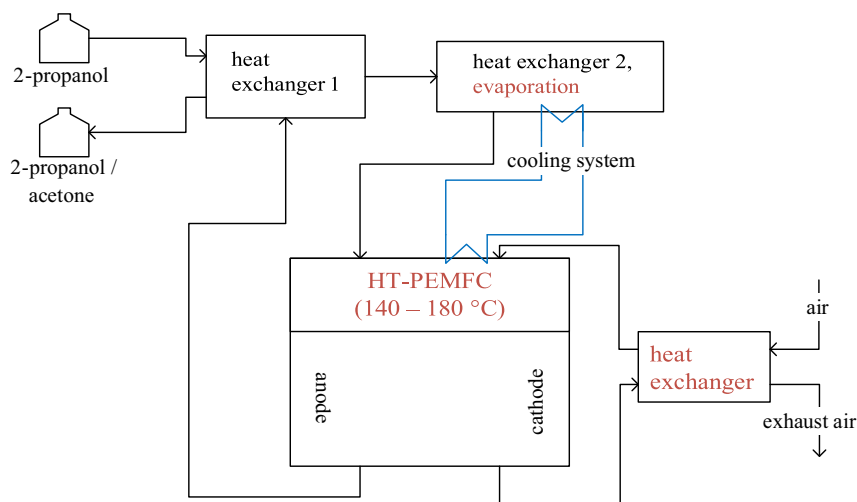


Figure 11. Flowchart including the main components for a direct fuel cell—HT-PEMFC with gaseous 2-propanol feed.

electrolyte membranes operated with hydrogen in the 140–180 °C range.^[9]

Aili et al. showed an important degradation mechanism when using methanol in a direct fuel cell with phosphoric-acid-based electrolytes.^[35] The formation of methyl phosphates by direct

esterification of phosphoric acid was found. This leads to a drastic reduction in conductivity. When operating a direct 2-propanol fuel cell with a phosphoric-acid-doped membrane, the same problem is to be expected, as the ester formation mechanism is expected to be similar with 2-propanol. In accordance with

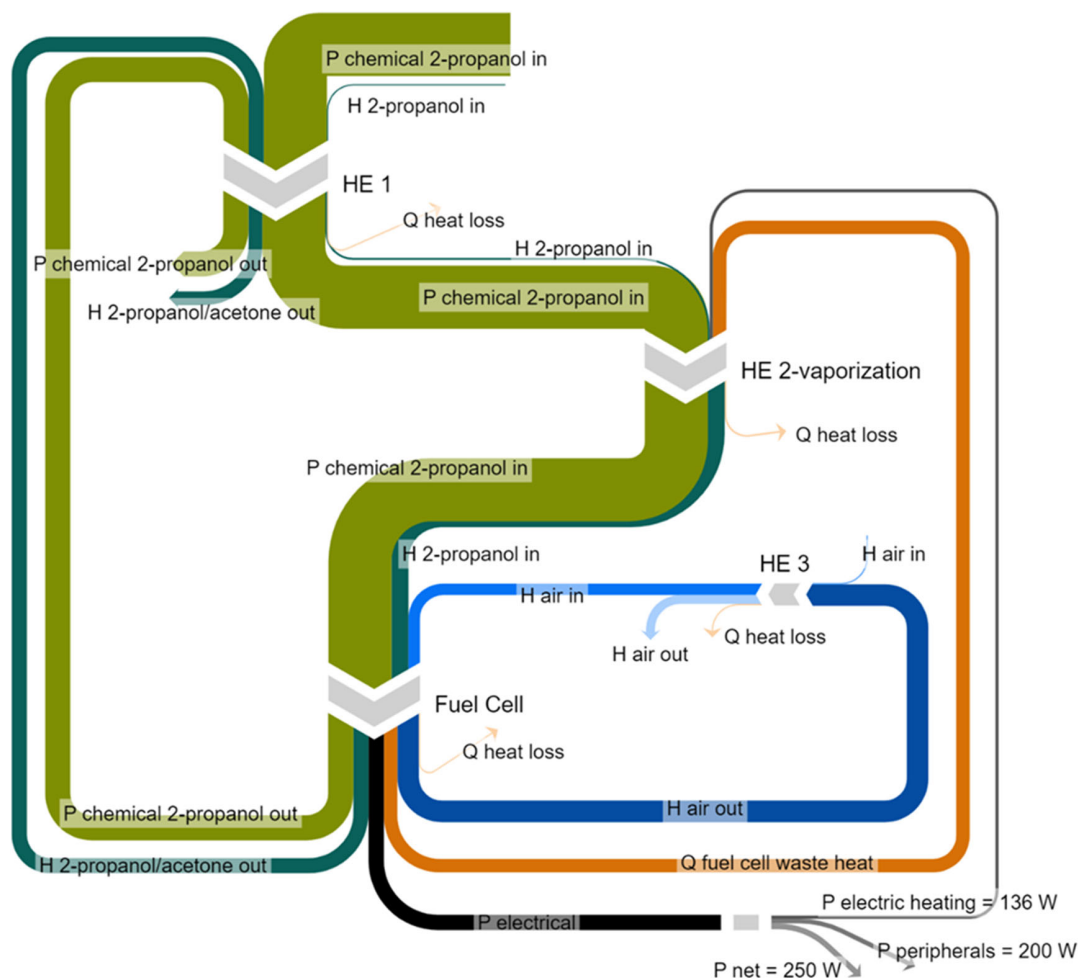


Figure 12. Energy flowchart of the whole system for a direct high-temperature fuel cell with the components heat exchanger 1 (HE1) and heat exchanger 2 (HE2-vaporization) for the anode feed, heat exchanger 3 (HE3) for the cathode feed, and fuel cell.

the literature, we propose the use of thermally cross-linked polybenzimidazole to improve the performance. Søndergaard et al. showed improved acid retention of the cross-linked membrane and thus significantly lower degradation rates.^[36]

3.2. Dehydrogenation of 2-Propanol Combined with HT-PEMFC

After analyzing the direct fuel cell scenarios, we will compare them with the two-step scenario, in which the 2-propanol is dehydrogenated in the first step and the released hydrogen is fed to a fuel cell in the second step. From the analysis of the previous scenarios of a direct fuel cell system, it can be concluded that only using the LT-PEMFC with a gaseous phase is technically feasible. From a thermodynamic point of view, three critical key aspects have been worked out: 1) There must be waste heat from the fuel cell. The exhaust gas of the fuel is not enough for the evaporation of the fuel. 2) The temperature gradient between the heat source and the target temperature of the evaporated fuel must be high enough. 3) The less water is in the system, the better the energy balance is.

Therefore, the focus of the two-step scenarios in this work was on the combination of hydrogen release from 2-propanol with a high-temperature hydrogen fuel cell. Equation (23) shows the dehydrogenation reaction.



Acetone and hydrogen are products. Acetone is collected in a tank and hydrogen is used for electrification in the high-temperature fuel cell. The chemical reaction in the cell proceeds according to Equation (4).

A fuel cell efficiency of 60% was assumed for the hydrogen fuel cell.^[28] In addition, the fuel utilization was set to 95%, and a recirculation of the hydrogen was assumed.

This means that 5% of the hydrogen remains unused due to crossover or purge losses. In steady-state operation, stoichiometry has no influence on the energy balance of the fuel cell, as we assumed that the hydrogen leaving the anode is returned to the anode inlet and enters the cell with the same enthalpy as it leaves it. Only the amount of hydrogen that is converted in the cell is relevant for the energy balance of the cell.

3.2.1. Thermochemical Dehydrogenation plus HT-PEMFC

This scenario contains a dehydrogenation unit in which the hydrogen is released from the 2-propanol and then fed to a high-temperature fuel cell. The hydrogen is separated from the 2-propanol/acetone mixture by cooling the mixture until condensation of 2-propanol and acetone occurs. This can be done in a heat exchanger to heat the 2-propanol feed for dehydrogenation. The heat of evaporation and dehydrogenation should be provided by the waste heat of the fuel cell. **Figure 13** shows the flowchart.

To model the dehydrogenation system, the inlet and outlet mass flow and the dehydrogenation enthalpy had to be determined.

The equilibrium conversion of the dehydrogenation of 2-propanol to acetone was simulated with the chemical process software Aspen Plus (version V10).^[37] The predictive Redlich Kwong-Soave (PSRK) property method was selected according to the guidelines of the Aspen Plus manual.^[38] PSRK is recommended for gas processing, refinery, and petrochemical applications. The simulations were carried out for the temperature range of 0–300 °C, a total pressure of 1 bar, and a pure 2-propanol feed.

The process flowsheet included the main feed stream containing pure 2-propanol fed into an “RGibbs”-type reactor, which is based on the minimization of Gibbs free energy approach to convergence calculations (**Figure 14**). No reaction equations were

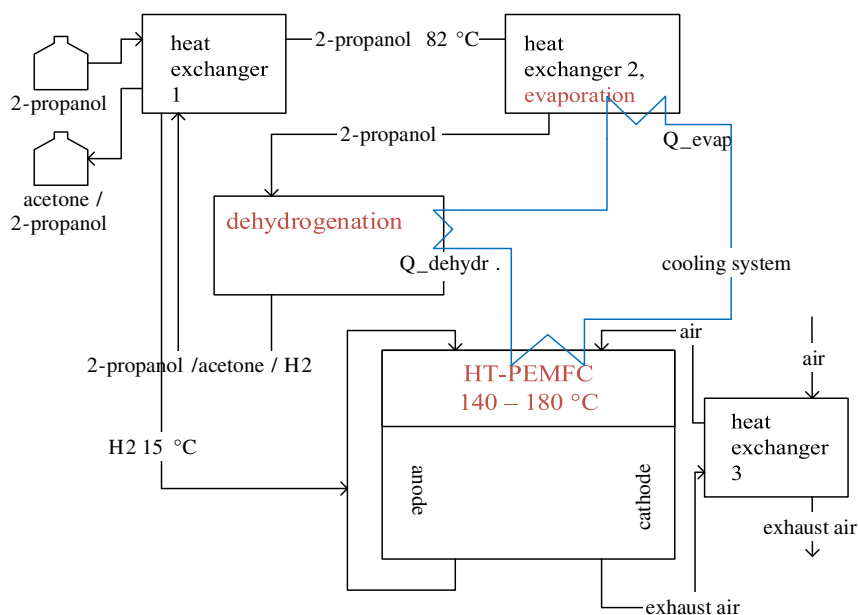


Figure 13. Flowchart including the main components for a thermochemical dehydrogenation of 2-propanol in combination with a hydrogen high-temperature fuel cell.

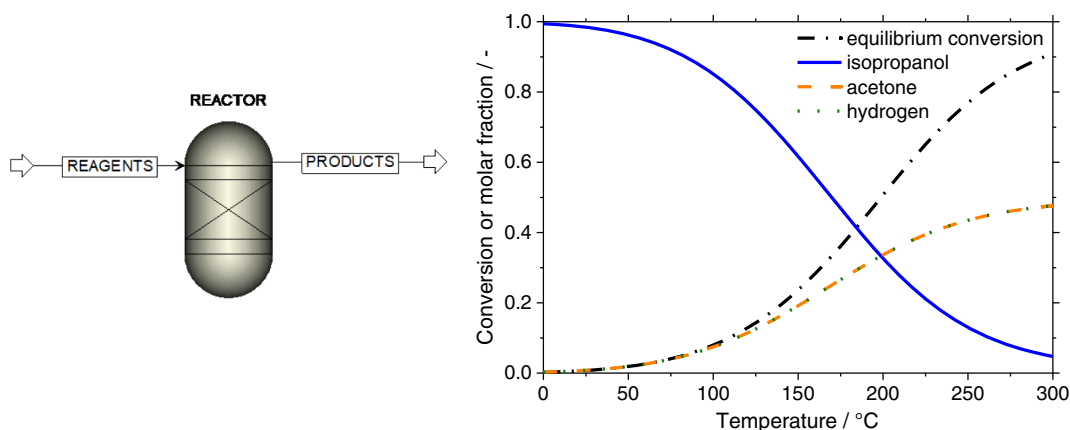


Figure 14. Main flowsheet of the simulation performed in Aspen Plus software. The feed stream consists of pure 2-propanol at 100 °C and 1 bar flowing into an RGibbs-type reactor at 1 kmol h⁻¹. The reactor operates at 100 °C and 1 bar. Here all potential reactions involving 2-propanol, H₂ and acetone can take place. (left) Equilibrium conversion and molar fractions of the dehydrogenation of 2-propanol to acetone at 1 bar as simulated using the Aspen Plus software. (right).

provided. Instead, only the compounds expected for different assumptions were defined in the outlet stream of the reactor, namely 2-propanol, H₂, and acetone.

The dehydrogenation enthalpy is calculated by computing the formation enthalpy differences between reactants and products. 2-propanol reacts to acetone and hydrogen according to Equation (23).

The formation enthalpy difference is calculated as followed

$$\Delta \hat{h} = \hat{h}_{f,acetone}^0 + \hat{h}_{f,hydrogen}^0 - \hat{h}_{f,2-propanol}^0 \quad (24)$$

The enthalpy of dehydrogenation must be provided in the form of heat. The only way to do this is to use the waste heat from the fuel cell. This limits the dehydrogenation temperature to temperatures lower than the operating temperature of the fuel cell. Otherwise, no heat transfer would be possible. Since the conversion increases with increasing temperature, the aim is to select the highest possible dehydrogenation temperature. The high-temperature fuel cell can be operated at a maximum of 180 °C.^[9]

To maintain a certain temperature gradient for the heat transfer, 175 °C is selected as the dehydrogenation temperature. In addition to the dehydrogenation enthalpy, there is also a heat demand for the evaporation of the fuel to reach the temperature level of the dehydrogenation process. The only heat source in the system is the high-temperature fuel cell. The waste heat of the fuel cell is independent of the dehydrogenation temperature because the hydrogen is cooled before being fed into the cell.

As already explained, the high-temperature fuel cell does not need to be humidified, as conductivity is ensured by phosphoric acid.

The flow diagram below shows the energy flow in the entire system (Figure 15).

It can be seen that the waste heat (305 W) is not sufficient for dehydrogenation. This means that there is still a heat requirement for the evaporation of the 2-propanol. Additional heat must therefore be supplied from outside.

As this concept does not work at the highest possible temperature, it will not work at lower temperatures either, as the

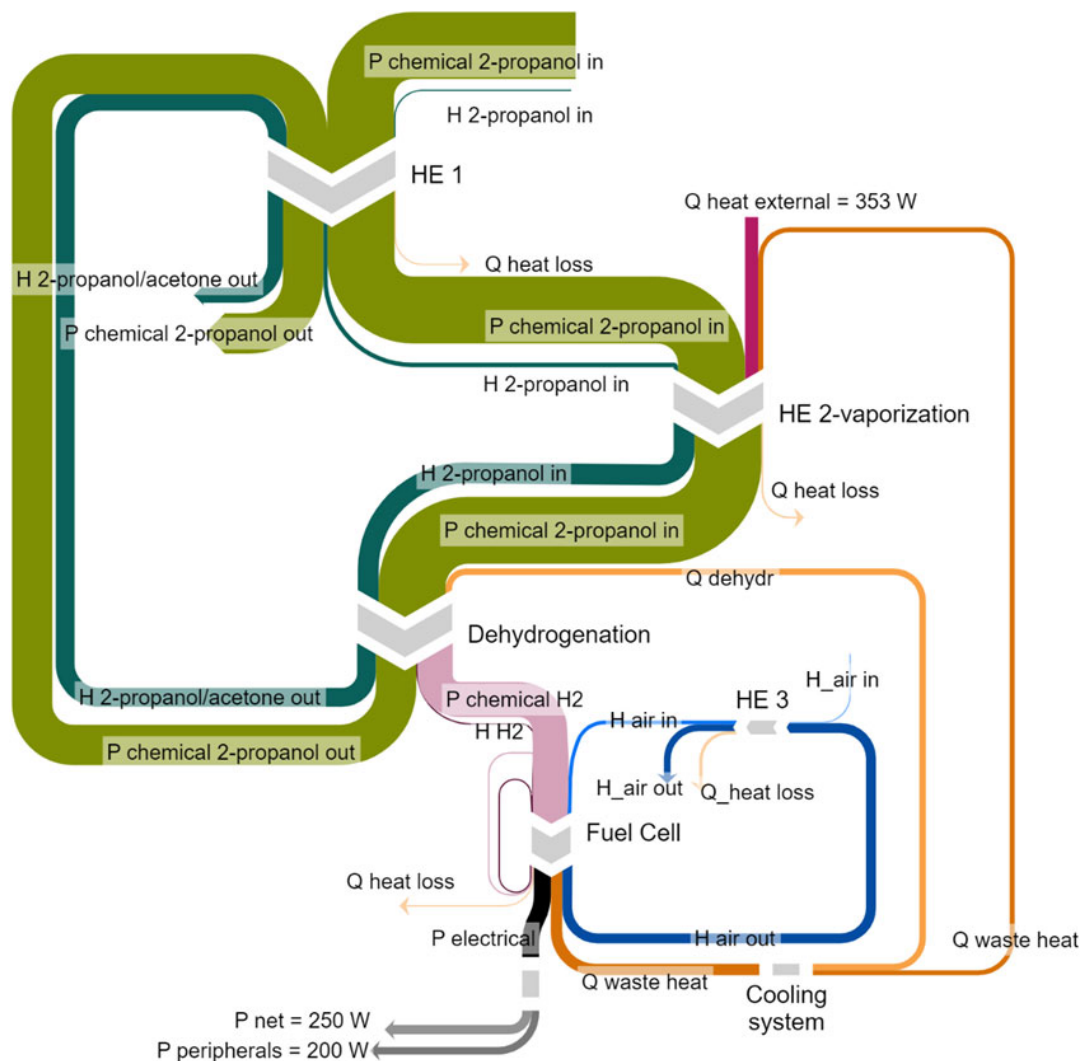


Figure 15. Energy flowchart of the whole system with the components heat exchanger 1 (HE1) and evaporator (HE2-vaporization) for the 2-propanol, dehydrogenation for releasing the hydrogen, fuel cell, and heat exchanger 3 (HE3) for the cathode feed.

$$E_{\text{Nernst}} = \frac{R \cdot T}{n \cdot F} \cdot \ln \left(\frac{p_{\text{out}}}{p_{\text{in}}} \right) \quad (26)$$

Taking the ohmic losses into account, the EHC voltage can be given according to ref. [40] as follows

$$E_{\text{EHC}} = E_{\text{Nernst}} + E_{\text{ohmic}} \quad (27)$$

$$\text{with } E_{\text{ohmic}} = I \times R = I \times \frac{ASR}{A_{\text{mem}}} \quad (28)$$

$$\text{Area – specific resistance } ASR = 0.3 \Omega \text{ cm}^2 \quad (29)$$

$$\text{Membrane area } A_{\text{mem}} = \frac{I}{j} = \frac{I}{0.3 \frac{\text{A}}{\text{cm}^2}} \quad (30)$$

$$\text{Current density } j = 0.3 \frac{\text{A}}{\text{cm}^2} \quad (31)$$

This leads to the following power demand

$$P_{\text{EHC}} = E_{\text{EHC}} \times I \quad (32)$$

The hydrogen leaving the EHC is humidified. Therefore, it must be cooled and, if necessary, passed through a separator to remove water or other substances present in the hydrogen due to crossover before entering the fuel cell. The outlet pressure of the EHC is set to 1.5 bar. On the anode side of the fuel cell, 5% of the injected hydrogen is expected to recirculate. Since the hydrogen is under pressure, the cathode air inlet must also be under pressure. Part of the required power can be taken from the expander, the remaining power must be obtained from the power generated by the fuel cell. After compression, the air inlet is heated in a third heat exchanger by transferring heat from the cathode air outlet.

The high-temperature fuel cell was modeled as in the previous scenario. Regarding water management, it is assumed that the water entering the air is removed with the air at the cathode outlet. In addition, all product water is discharged at the cathode. It is assumed that there is no diffusion to the anode side.

The simulation results show that the fuel can be heated and vaporized by the anode exhaust gas and by recovering the waste heat from the fuel cell. The exhaust air can be used to heat the air inlet of the fuel cell. At the target fuel cell net power of 250 W (considering the EHC and compressor as additional loads besides the previously assumed peripherals), the EHC requires 72.96 W. The compressor consumes 19.47 W (the expander power has already been subtracted). This results in system efficiency of 0.29.

Provided that the energy balance of the system is positive, other operating points are also possible. Based on the assumptions of Table 1, the fuel cell can be operated in the range of 140 to 180 °C. A lower fuel utilization of 55% in the EHC still results in a positive energy balance at a fuel cell temperature range of 140 to 180 °C. This utilization is then comparable to the direct 2-propanol fuel cell.

The diagram below shows the enthalpy flows, heat flows, and converted electrical as well as chemical power in the system at 160 °C with a utilization of 80% in the electrochemical conversion unit and a fuel cell stoichiometry of 2.5 (Figure 17).

It is obvious that the chemical power provided by the 2-propanol is quite high compared to the enthalpy flows. As in the concepts before, there is a heat loss from each component, but most of the input follows the main flow and can partially be converted to electric energy. No external heat is needed. All waste heat can be used quite efficiently.

In summary, this concept represents a thermodynamically efficient way to use 2-propanol in combination with a high-temperature fuel cell. From a technical point of view, an HT-PEMFC technology with a sufficiently high level of technological maturity is available for application. Initial experiments on the direct electrochemical conversion of isopropanol to acetone and hydrogen in an electrochemical hydrogen compressor show promising results, which make this option appear feasible and quite attractive. Obviously, the optimization of the direct electrochemical conversion of isopropanol beyond the performance data considered here would make the concept even more appealing.

4. Discussion and Conclusion

A comparison of the concepts studied reveals that there are some key elements that determine whether the targeted net power can be achieved or not. The main findings are summarized in Table 2.

First, the evaporation of 2-propanol means a high heat demand, which must be covered by the power released in the cells—either in the form of heat or in the form of electricity. Obviously, the most efficient way is to recover as much heat as possible. There are two heat sources available: the cooling circuit and the hot exhaust gases. Both strategies require a sufficiently significant temperature gradient to transfer the heat to the 2-propanol. Both heat sources are at approximately the same temperature level as the fuel cell. Heat recovery from one of the two sources alone can, therefore, only achieve an inlet temperature that is cooler than the operating temperature of the fuel cell. Otherwise, there would be no temperature gradient in the heat exchanger. A cooler inlet means that some of the heat generated by the reaction is already needed to heat the fuel cell inlet. Therefore, the waste heat is not as high as one might expect.

In concepts where water has to be evaporated in addition to 2-propanol, this is even more critical because much more heat energy is needed. Water not only adds mass to the system but also has a much higher enthalpy of vaporization than 2-propanol, so the amount of water has a strong influence on the energy balance.

All of the aforementioned challenges could be counteracted by recirculating the anode isopropanol/acetone flow. So far, there is not enough data for a realistic system layout with recirculation. Especially the influence of acetone content and the power density is important. Without that knowledge, studies would be biased by the assumptions.

At the cathode supply, we can see that less humidification leads to a more positive energy balance. The enthalpy of the humid air increases over-proportionally with increasing temperature, which results in the exit enthalpies being significantly higher than the entry enthalpies of the air.

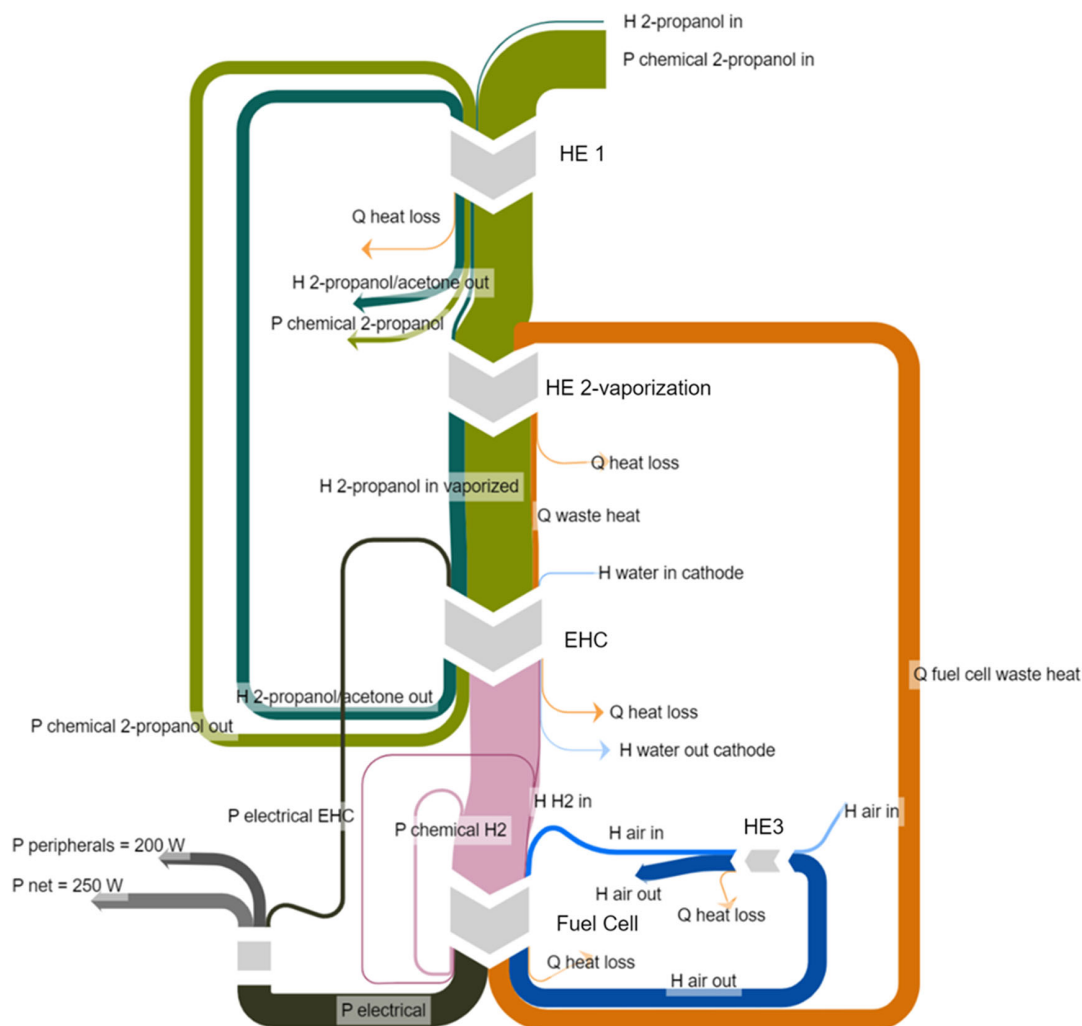


Figure 17. Energy flowchart of the whole system for the electrochemical 2-propanol to hydrogen conversion with the components heat exchanger 1 (HE1) and evaporator (HE2-vaporization) for the anode feed, electrochemical hydrogen compressor (EHC), fuel cell, and heat exchanger 3 (HE3) for the cathode feed.

Stoichiometry has a significant influence on the energy balance of the fuel cell as well. High air mass flows can transport more water out of the cell than low ones. If water is lost, it must be supplied again to keep the membrane humidified. If the water is not supplied in gaseous form, it cools the fuel cell by evaporation. From a thermodynamic point of view, it is better to have less water in the cell. In this study, we assumed the necessary humidification of 100% for the inlet air. If the relationship between the water content of the membrane and the power density were modeled more accurately, it would probably be possible to find efficient operating points with less than 100% relative humidity.

Fuel utilization is another important factor. With low utilization, a large amount of fuel is pushed through the system without participating in the reaction but must also be heated and vaporized. Low utilization is not only bad for power density but also a problem from a thermodynamic point of view. Thus, higher fuel utilization is a very effective way to push the efficiency of all concepts that use evaporated fuel. Note, that we have assumed

a fuel utilization of 55% in this study for all 2-propanol direct fuel cell concepts. Our current laboratory research targets significantly higher levels of fuel utilization.

As far as the direct 2-propanol fuel cell is concerned, the first concept with a low-temperature fuel cell and liquid fuel is promising from a thermodynamic point of view if the water feed and the stoichiometry are reduced compared to the model assumptions made. The main advantages of the first concept are the elimination of evaporation of the fuel and air humidification. However, technical feasibility has not been achieved yet. Operation in the liquid form leads to the destruction of the currently applied MEA membrane. Thus, novel ionomer binders are required that are chemically stable in the presence of 2-propanol and acetone. Operation of a low-temperature fuel cell in the gaseous phase is not feasible thermodynamically with a heat deficit of 1.5 times the net power of 250 W. The high technological maturity of LT-PEMFCs would be advantageous. Operation of a middle-temperature fuel cell is not feasible thermodynamically

Table 2. Summary of the main benefits and problems of all analyzed scenarios.

			Main benefits	Main problems/disadvantages
Direct fuel cell (one-step scenario)	Liquid	LT-PEMFC	No evaporation required No humidification required Net power of 250 W achieved	Destruction of the MEA in 2- molar solutions Too much water in the system Lower stoichiometry for less water output required Low utilization
	Gaseous	LT-PEMFC	High technology readiness level	Heat requirement for evaporation Very low-temperature gradient for evaporation of fuel
		MT-PEMFC	Higher temperature gradient than LT- PEMFC	Heat demand for evaporation Low relative humidity → low power density Outlet flows with a high enthalpy
		HT-PEMFC	Small amount of water in the system Sufficient heat for evaporation of the fuel Net power of 250 W can be achieved	Degradation due to esterification expected
Dehydrogenation + hydrogen fuel cell (two-step scenario)	Thermochemical dehydrogenation	Pure 2-propanol as anode feed No humidification of HT- PEMFC required Hydrogen HT- PEMFC: high technology readiness level	Heat requirement for evaporation of 2-propanol Low conversion during dehydrogenation at temperatures below the boiling point	
	Electrochemical 2-propanol to hydrogen conversion	High-temperature gradient between fuel cell and EHC Neat 2-propanol No humidification of HT- PEMFC Net power of 250 W can be reached Hydrogen HT- PEMFC: high technology readiness level	More peripheral components due to higher system pressure	

either, as the heat deficit in this scenario is many times the heat deficit of the low-temperature fuel cell, caused by a large amount of water leaving the fuel cell. From a technical point of view, MT-PEMFCs are a current area of research struggling with much lower efficiency than current LT-PEMFCs. In the case of a high-temperature direct fuel cell with gaseous 2-propanol, there are problems with the formation of phosphate esters through direct esterification of phosphoric acid, which is used for the membranes in high-temperature fuel cells. However, the heat integration can be made efficient due to a high-temperature gradient between fuel cell and evaporator as well as the low water content in the system.

A look at the two-step scenarios reveals one main benefit for both concepts: the use of a hydrogen HT-PEMFC, which has a high technology readiness level and needs no humidification. However, in the first scenario, which involves an evaporator and the dehydrogenation of 2-propanol in a reactor, the heat demand is too high, so the concept does not lead to a self-sufficient system. Dehydrogenation at a temperature close to the fuel cell temperature leads to a heat deficit for evaporation, while dehydrogenation in the liquid phase entails too little conversion of 2-propanol into hydrogen.

In contrast, the electrochemical 2-propanol to hydrogen conversion leads to an efficient system. The utilization of fuel is significantly higher in the EHC than in the dehydrogenation reactor. Moreover, due to the temperature gradient between the fuel cell and the EHC, sufficient heat can be transferred for vaporization. A disadvantage could be the more complex system, as components such as a compressor and expander are required to achieve a higher system pressure.

Of all the concepts studied, the electrochemical 2-propanol to hydrogen conversion seems to be the one with the highest (thermodynamic and technical) feasibility. Apart from that, a low-temperature direct fuel cell in the liquid phase and a high-temperature direct fuel cell in the gaseous phase show thermodynamic feasibility, although both have a lower system efficiency than the two-step scenario previously mentioned and there are technical issues that still need to be solved.

This article shows how crucial it is to evaluate future fuel cell systems not only according to technical feasibility and maximum power density but also from a thermodynamic point of view. From concrete scenarios, it was possible to derive generally valid relationships that are fundamental for the design of a fuel cell system. As some of our assumptions are conservative and may be improved by further research (e.g., fuel utilization in fuel cells, conversion efficiency), the current study represents a scenario-based system analysis that can also help guide future research efforts with the intention of improving the electrification of liquid organic hydrogen carrier systems.

Acknowledgements

This work was partly funded by the Bavarian Ministry of Economic Affairs, Regional Development, and Energy. This work was partly carried out as part of the FCS-HD project, which is funded by the German Federal Ministry of Digital and Transport as part of the National Hydrogen and Fuel Cell Technology Innovation Programme. The funding directive is coordinated by NOW GmbH and implemented by Project Management Jülich (PtJ).

Open Access funding enabled and organized by Projekt DEAL.

Conflict of Interest

The authors declare no conflict of interest.

Data Availability Statement

The data that support the findings of this study are available from the corresponding author upon reasonable request.

Keywords

2-propanol fuel cell system, balance of plant, energy balancing, system integration, technical integration

Received: April 5, 2022

Revised: May 23, 2022

Published online:

- [1] K. Müller, S. Thiele, P. Wasserscheid, *Energy Fuels* **2019**, *33*, 10324.
- [2] K. Gärtner, Friedrich-Alexander-Universität Erlangen-Nürnberg, Doctoral Dissertation/PhD Thesis **2018**.
- [3] M. Brodt, K. Müller, J. Kerres, I. Katsounaros, K. Mayrhofer, P. Preuster, P. Wasserscheid, S. Thiele, *Energy Technol.* **2021**, *9*, 2100164.
- [4] N. Kariya, A. Fukuoka, M. Ichikawa, *Phys. Chem. Chem. Phys.* **2006**, *8*, 1724.
- [5] A. Rahman, *Bull. Chem. React. Eng. Catal* **2011**, *5*, 113.
- [6] G. Sievi, D. Geburtig, T. Skeledzic, A. Bösmann, P. Preuster, O. Brummel, F. Waidhas, M. A. Montero, P. Khanipour, I. Katsounaros, J. Libuda, K. J. J. Mayrhofer, P. Wasserscheid, *Energy Environ. Sci.* **2019**, *12* 2305.
- [7] P. Hauenstein, D. Seeberger, P. Wasserscheid, S. Thiele, *Electrochem. Commun.* **2020**, *118*, 106786.
- [8] P. Hauenstein, I. Mangoufis-Giasin, D. Seeberger, P. Wasserscheid, K. J. Mayrhofer, I. Katsounaros, S. Thiele, *J. Power Sources Adv.* **2021**, *10*, 100064.
- [9] K.-S. Lee, J. S. Spindelov, Y.-K. Choe, C. Fujimoto, Y. S. Kim, *Nat. Energy* **2016**, *1*, 16120.
- [10] A. Kusoglu, A. Z. Weber, *Chem Rev* **2017**, *117*, 987.
- [11] S. S. Araya, F. Zhou, V. Liso, S. L. Sahlin, J. R. Vang, S. Thomas, X. Gao, C. Jeppesen, S. K. Kær, *Int. J. Hydrogen Energy* **2016**, *41*, 21310.
- [12] V. Ramani, H. Kunz, J. Fenton, *J. Membr. Sci.* **2004**, *232*, 31.
- [13] P. Antonucci, A. Aricò, *Solid State Ion.* **1999**, *125*, 431.
- [14] K. T. Adjemian, R. Dominey, L. Krishnan, H. Ota, P. Majsztrik, T. Zhang, J. Mann, B. Kirby, L. Gatto, M. Velo-Simpson, J. Leahy, S. Srinivasan, J. B. Benziger, A. B. Bocarsly, *Chem. Mater.* **2006**, *18*, 2238.
- [15] M. Breitwieser, C. Klose, M. Klingele, A. Hartmann, J. Erben, H. Cho, J. Kerres, R. Zengerle, S. Thiele, *J. Power Sources* **2017**, *337*, 137.
- [16] W. Zorn, Geschwindigkeit und Leistung auf Fahrrädern Berechnen, **2022**, <http://www.kreuzotter.de/deutsch/speed.htm> (accessed: September 2021).
- [17] R. P. O'Hayre, S.-W. Cha, W. G. Colella, F. B. Prinz, in *Fuel Cell Fundamentals*, John Wiley & Sons Inc, Hoboken NJ **2016**.
- [18] O. Berger, Thermodynamische Analyse eines Brennstoffzellensystems zum Antrieb von Kraftfahrzeugen, Doctoral dissertation, Universität Duisburg-Essen **2009**.
- [19] P. Linstrom, in *NIST Chemistry WebBook, NIST Standard Reference Database 69*, National Institute of Standards and Technology, Gaithersburg, MD **1997**.
- [20] P. von Böckh, M. Stripf, in *Technische Thermodynamik*, Springer, Berlin **2015**.
- [21] M. Huber, A. Harvey, E. Lemmon, G. Hardin, I. Bell, M. McLinden, in *NIST Reference Fluid Thermodynamic And Transport Properties Database (REFPROP) Version 10 – SRD 23*, National Institute of Standards and Technology, Gaithersburg, MD **2018**.
- [22] M. Eikerling, A. A. Kornyshev, A. R. Kucernak, *Phys. Today* **2006**, *59*, 38.
- [23] H. S. Lee, in *Thermal Design Heat Sinks, Thermoelectrics, Heat Pipes, Compact Heat Exchangers, And Solar Cells*, John Wiley & Sons, Hoboken **2010**.
- [24] P. Böckh, W. T. Wärmeübertragung, *Wärmeübertragung - Grundlagen und Praxis*, Springer Berlin Heidelberg, Heidelberg **2015**.
- [25] R. Huizing, in Design and Membrane Selection for Gas to Gas Humidifiers for Fuel Cell Applications thesis for degree of Master of applied science in chemical engineering, University of Waterloo **2007**.
- [26] D. Chen, H. Peng, *J. Dyn. Syst. Measur. Control* **2005**, *127*, 424.
- [27] N. Ahsan, A. Al Rashid, A. A. Zaidi, R. Imran, S. A. Qadir, *Energy Rep.* **2021**, *7*, 2635.
- [28] O. Bethoux, *Energies* **2020**, *13*, 5843.
- [29] G. Sievi, in *Elektrochemische Oxidation Von 2-Propanol In Einer Direkt-Brennstoffzelle*, Friedrich-Alexander-Universität Erlangen-Nürnberg, Erlangen, Germany **2020**.
- [30] D. Cao, S. H. Bergens, *J. Power Sources* **2003**, *124*, 12.
- [31] M. L. Perry, Z. Yang, *J. Electrochem. Soc.* **2019**, *166*, F3268.
- [32] Dortmund Data Bank, <http://www.ddbst.de/en/EED/VLE/VLE%202-Propanol%3BWater.php> (accessed: September 2021).
- [33] N. Wehkamp, M. Breitwieser, A. Büchler, M. Klingele, R. Zengerle, S. Thiele, *RSC Adv.* **2016**, *6*, 24261.
- [34] C. Klose, M. Breitwieser, S. Vierrath, M. Klingele, H. Cho, A. Büchler, J. Kerres, S. Thiele, *J. Power Sources* **2017**, *361*, 237.
- [35] D. Aili, A. Vassiliev, J. O. Jensen, T. J. Schmidt, Q. Li, *J. Power Sources* **2015**, *279*, 517.
- [36] T. Søndergaard, L. N. Cleemann, H. Becker, D. Aili, T. Steenberg, H. A. Hjuler, L. Seerup, Q. Li, J. O. Jensen, *J. Power Sources* **2017**, *342*, 570.
- [37] aspenONE Engineering, *AspenPlus*, Aspen Technology **2017**.
- [38] Aspen Technology, *Aspen Plus Manual*, Aspen Technology, Burlington **2017**.
- [39] S. Mrusek, P. Preuster, K. Müller, A. Bösmann, P. Wasserscheid, *Int. J. Hydrogen Energy* **2021**, *46*, 15624.
- [40] B. L. Kee, D. Curran, H. Zhu, R. J. Braun, S. C. DeCaluwe, R. J. Kee, S. Ricote, *Membranes* **2019**, *9*, 77.